Acoustic sensor performance in coastal waters: solid suspensions and bubbles

S. D. Richards[1], T. G. Leighton[2]

[1] Defence Evaluation and Research Agency, DERA Winfrith, Winfrith Technology Centre, Dorchester, Dorset, DT2 8XJ, UK. sdrichards@dera.gov.uk
[2] Institute of Sound and Vibration Research, University of Southampton, Highfield, Southampton, SO17 1BJ, UK. tgl@isvr.soton.ac.uk

Abstract

Coastal waters may be characterised by depth-dependent populations of suspended solid particles and microbubbles. These populations may be acoustically significant in that they may modify the complex wavenumber for compression waves, increasing the volume attenuation and altering the phase speed. These effects have been incorporated into a ray-based sonar model and results are presented which show that they may have a significant effect on the performance of high frequency acoustic sensors in coastal waters. The application of this work to acoustical oceanography is illustrated by means of a speculative proposal to use trans-estuarine transmission measurements to monitor suspended sediment load.

1. Introduction

Coastal environments may be characterised by suspensions of solid mineral particles, stirred up as a result of wave action or currents generated by wind and tide, or entering the coastal environment in river outflows. Littoral waters may also contain significant populations of microbubbles throughout the water column, which may be surface generated or rising from the seabed where they result from bio-chemical processes. Both suspended solid particles and microbubbles may have a significant influence on the acoustic properties of the medium, modifying the complex wavenumber. It is therefore important to quantify their effects on the performance of acoustic sensors operating in turbid and bubbly environments, including active sonar systems, echosounders, acoustic Doppler current profilers, and acoustic sensors designed for measuring solid particle or bubble populations.

2. Particulate suspensions

2.1 Introduction

The presence of suspended particulate matter in the water column leads to additional acoustic attenuation through the processes of thermal and visco-inertial absorption and scattering. These effects may be important over the range of frequencies typically employed by high frequency acoustic sensors (tens of kHz to several MHz) and over the range of particle sizes typically found in suspension in coastal waters (sub-micron to hundreds of microns). For this frequency and particle size range, the following generally apply for typical marine mineral particles. First, thermal absorption may be neglected. Second, visco-inertial absorption is the dominant loss mechanism, with scattering becoming important at the upper extremes of particle size and frequency. Third, the effect of suspended mineral particles on the sound speed is small, and may therefore be neglected.

2.2 Attenuation coefficient

The additional contribution to the plane wave attenuation coefficient due to a suspension of solid particles, neglecting thermal absorption, may be written

$$\alpha_p = \alpha_v + \alpha_s \tag{1}$$

where the subscripts *v* and *s* refer to the visco-inertial absorption and scattering contributions respectively.

For dilute suspensions the visco-inertial absorption coefficient is given by [1]

$$\alpha_v = \frac{\varepsilon k(\sigma-1)^2}{2}\left[\frac{s}{s^2+(\sigma+\tau)^2}\right] \tag{2}$$

where ε is the volume fraction of suspended particles, *k* is the acoustic wavenumber, σ is the fluid-solid density ratio, and τ and *s* are, respectively, the coefficients of the inertial and drag terms in the equation for the force acting on the particles (see [1]).

TG Leighton, GJ Heald, HD Griffiths, G Griffiths, (eds.), 'Acoustical Oceanography', Proc. Institute of Acoustics Vol. 23 Part 2, 2001.

The attenuation due to scattering by suspended particles may be determined using the common high-pass approximation [2]

$$\alpha_s = \frac{\varepsilon K_\alpha x^4}{a\left(\frac{4}{3}K_\alpha x^4 + \xi x^2 + 1\right)} \tag{3}$$

where a is the particle radius, $x=ka$ is the dimensionless size parameter, K_α contains the dependence on density and compressibility contrasts (see [2]) and ξ is a free parameter controlling the behaviour of the function for intermediate values of x between the Rayleigh (small x) and geometric (large x) regimes.

3. Microbubbles

3.1 Introduction

As with solid particles, the presence of microbubbles in the water column leads to additional acoustic attenuation through thermal and viscous absorption and scattering. Unlike particles, however, resonant scattering can be important in the case of bubbles, and the scattering cross-section of a bubble near resonance may be very much larger than its geometric cross-section. Bubbles also cause the compressibility of the medium to be complex, resulting in dispersion.

3.2 Dispersion relation

The dispersion relation for a bubbly liquid may be written [3]

$$k_b^2 = \frac{\omega^2}{c^2} + 4\pi\omega^2 \int_{a_0=0}^{\infty} \frac{a_0 n_b(a_0) da_0}{\omega_0^2 - \omega^2 + 2ib\omega} \tag{4}$$

where k_b is the complex wavenumber for the bubbly liquid, ω is the angular frequency of the acoustic wave, c is the speed of sound in the ambient fluid, a_0 is the equilibrium bubble radius and $n_b(a_0)da_0$ is the number of bubbles per unit volume in the size range a_0 to $a_0 + da_0$ (it is conventional to use $da_0 = 1\mu\text{m}$), ω_0 is the resonant frequency of bubbles having equilibrium radius a_0. The damping constant b is a summation of the viscous, thermal and radiation damping of the bubble, given by [3]

$$b = \frac{2\mu}{\rho a_0^2} + \frac{p_0}{2\rho a_0^2 \omega}\Im\Phi + \frac{\omega^2 a_0}{2c} \tag{5}$$

where ρ and μ are the density and shear viscosity of the ambient liquid, p_0 is the equilibrium gas pressure in the bubble and Φ is a thermal scaling factor.

The phase speed c_b and attenuation coefficient α_b for the bubbly liquid may be extracted from the real and imaginary parts of (4) using the following relation

$$k_b = \frac{\omega}{c_b} + i\alpha_b \tag{6}$$

4. Sonar performance model

4.1 Model description

Sonar performance calculations have been carried out using a ray-based environmental sonar model. This model computes ray paths in a horizontally stratified, range-independent environment assuming a linear sound speed gradient in each horizontal layer. The signal-to-noise ratio along each ray path is calculated using the active sonar equation, including the effects of geometric spreading; volume absorption; surface, bottom and volume reverberation; and various propagating and non-propagating noise contributions.

4.2 Model enhancements

The additional attenuation due to the presence of suspended particulate matter and microbubbles have been incorporated into the volume loss algorithm using equations (1) to (6), resulting in a total volume attenuation coefficient given by

$$\alpha = \alpha_w + \alpha_p + \alpha_b \tag{7}$$

where α_w is the physico-chemical absorption by clear seawater. Currently this has been implemented with a depth-dependent suspended sediment concentration profile and a depth-independent particle size distribution. The phase speed and additional attenuation contributions due to a fully depth-dependent bubble size spectrum are calculated using a depth-dependent version of the dispersion relation for bubbly liquids [7]. Several empirical expressions exist for calculating α_w, such as that of Fisher and Simmons [4], Thorpe [5] and Francois and Garrison [6].

The additional attenuation due to suspended solid particles and microbubbles in the water column has been included in the calculations of both the signal levels and the noise and reverberation levels in order to determine the resulting signal-to-noise ratio. The effect of the bubbles on the phase speed has been used to modify the sound speed profile used in computing the ray paths.

5. Results

5.1 Particulate suspensions

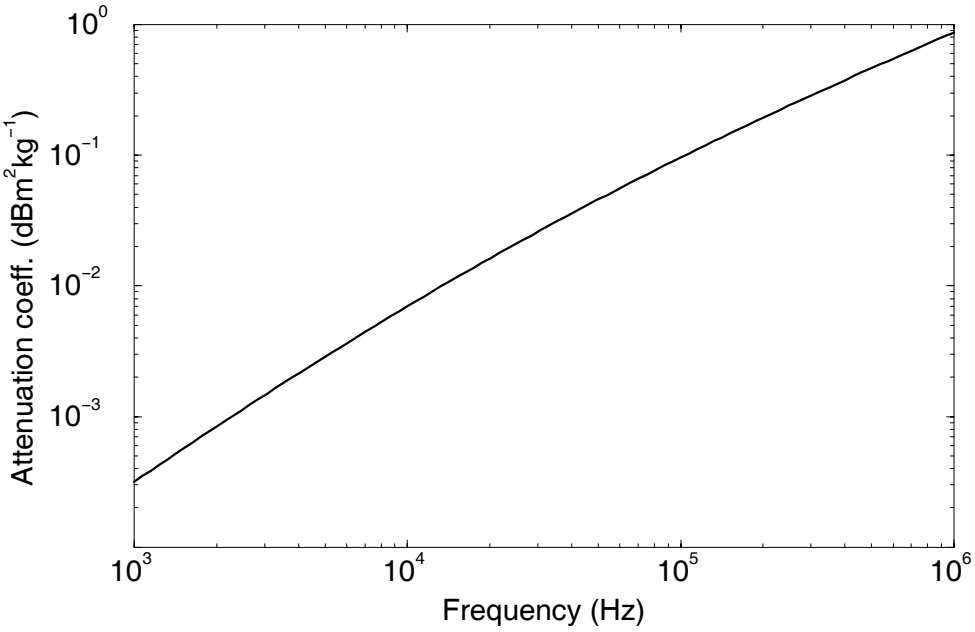

Figure 1. Calculated normalised excess attenuation spectrum for a dilute suspension of marine sediment particles.

Figure 1 shows the calculated attenuation coefficient for a suspension of fine, clay-like marine sediment particles, with radii ranging from less than 0.1 μm to more than 60 μm (modal radius around 2-3 μm). The attenuation spectrum was computed using (2) and (3) integrated over the particle size distribution, which was measured by laser diffraction analysis. The attenuation coefficient has been normalised with respect to total mass concentration, resulting in normalised units of dBm^2kg^{-1} ($=dBm^{-1}(kgm^{-3})^{-1}$). This figure shows that the attenuation coefficient is a smooth, monotonically increasing function of frequency for a typical fine marine suspension. The attenuation scales linearly with the volume fraction of suspended solids in the dilute regime (valid for most practical marine suspensions, except in the boundary layer near to the seabed). Consider, as a numerical example, a suspended sediment concentration of 0.1 kgm^{-3}, such as may be found in a turbid estuary, with an acoustic plane wave at a frequency of 100 kHz. The figure shows that this example results in an attenuation coefficient of around 0.01 dBm^{-1}, equating to an excess attenuation of several dB over a propagation range of a few hundred metres.

The calculations shown in Figure 1 compare favourably with laboratory measurements of viscous absorption by dilute suspensions of samples of this marine sediment over the limited frequency range 50-150 kHz [8]. It is thought [8] that the reasonable agreement between measurements made using natural, irregular particles and the predictions of a model based on spherical particles is a result of ensemble averaging over many particle sizes, shapes and orientations.

5.2 Microbubbles

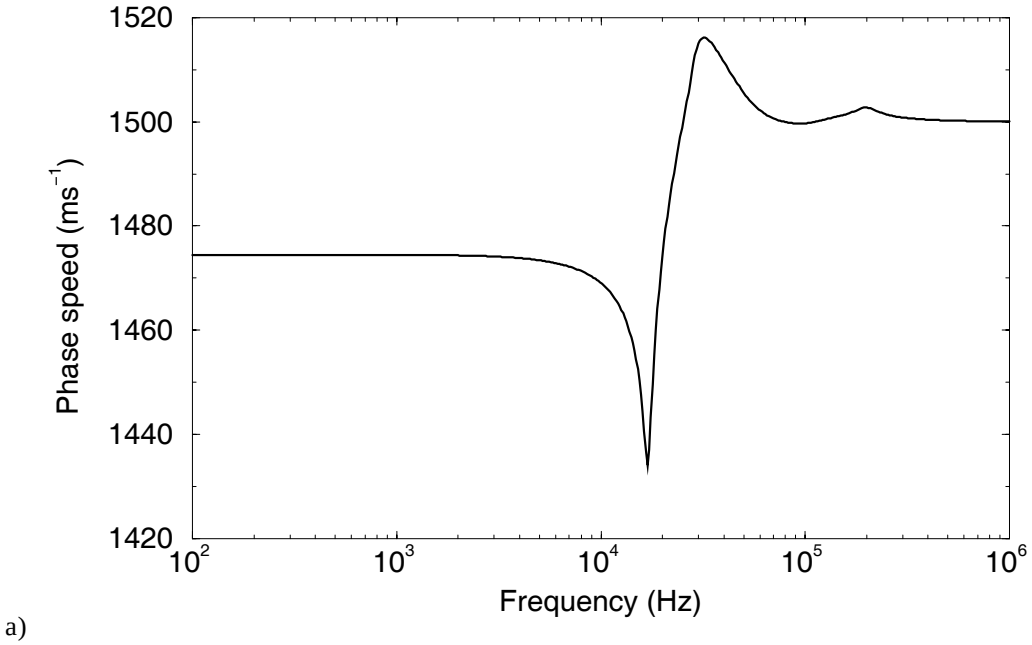

a)

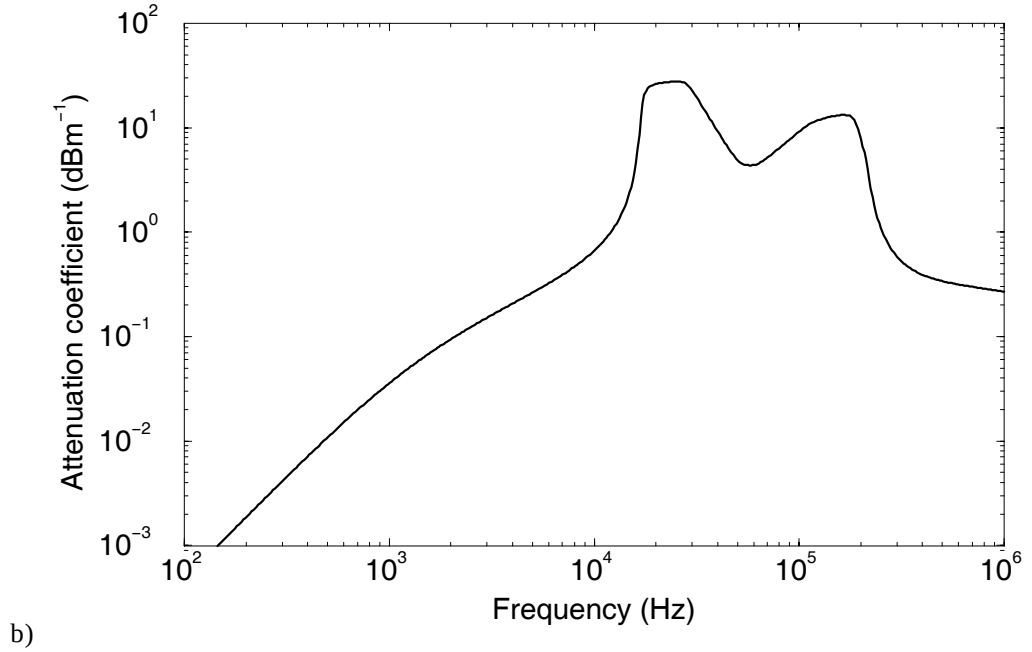

b)

Figure 2. a) Calculated phase speed variation with frequency for a bubble population measured at sea (at 0.5 m depth in 17-22 m of water, at windspeeds of 10-12 ms^{-1}). b) Calculated excess attenuation variation with frequency for this measured bubble population.

Figure 2 shows the phase speed (2a) and excess attenuation (2b) spectra calculated for a bubble population measured at sea using a combination frequency technique [9]. These figures were obtained using (4) to (6), with the integral with respect to bubble radius taken over the measured bubble population, which contained bubbles with equilibrium radii in the range 10μm to 200μm. For water containing a monodisperse bubble population there will be a rapid change in phase speed around the resonant frequency of the bubbles, with a corresponding attenuation peak resulting from the large radiation losses at resonance. Although Figure 2a shows the result of integrating over a natural distribution of bubble sizes, this behaviour of the phase speed is still evident. However,

this bubble population results in the bimodal attenuation spectrum shown in Figure 2b. These results show that, for the bubble population used, the presence of bubbles leads to significant variation in the phase speed, with strong dispersion over the frequency range 10 kHz to 40 kHz, and significantly different phase speeds above and below this frequency range. The results also show that large excess attenuation may be observed over a wide frequency range, with particularly high attenuation over the range 10 kHz to 300 kHz. The local minimum in the attenuation spectrum at around 60 kHz for this bubble population could be exploited to optimise acoustic sensor performance in this high attenuation band.

5.3 Sonar performance

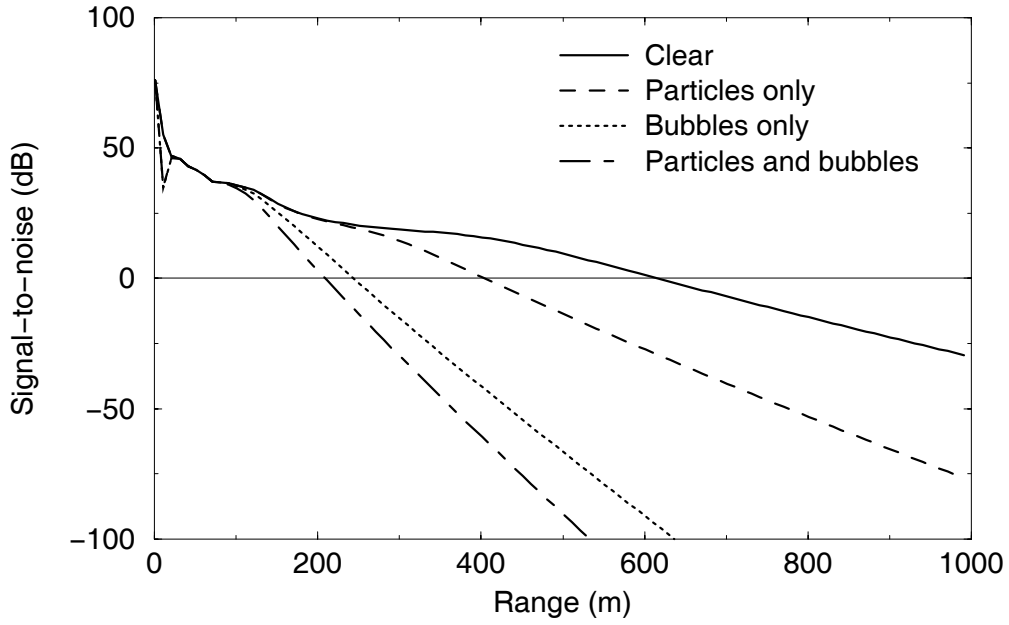

Figure 3. Computed signal-to-noise ratio, showing the effects of suspended solid particles and microbubbles (see text).

Figure 3 shows the computed signal-to-noise ratio for a typical high frequency, shallow water sonar scenario. In this example the water depth was 40 m, the bottom type was mud and the water column was isothermal. The horizontally looking, monostatic projector/receiver was at a depth of 20 m and the source frequency was 80 kHz. The calculations for water containing suspended solid particles assume a monodisperse population of particles with radius 2 μm, density 2600 kg m^{-3}, and a depth-independent concentration of 0.2 kg m^{-3}. A depth-dependent distribution [10] of microbubbles with equilibrium radii in the range 10-200 μm was used, with coefficients chosen to approximate at-sea bubble density measurements [11, 12]. This bubble population is appropriate for the persistent background bubble population in calm, isothermal coastal waters and not for conditions where there is a large surface-generated bubble population. Future calculations will be carried out using a bubble size spectrum appropriate for a surface generated population [13].

Taking a figure of merit of 0 dB (shown by the horizontal line in the figure) results in a detection range in clear water of about 615 m in this example. The additional attenuation due to the chosen population of suspended particles reduces this range to 403 m. The bubble population has an even greater effect, reducing the detection range to 243 m, whilst the combined effect of bubbles and suspended particles reduces the detection range to just 209 m.

5.4 Estuarine application

As an example of the application of this work to environmental measurements, a technique for monitoring the suspended sediment load flowing from a river mouth or estuary is speculatively proposed. Since the transmission loss between two points in turbid water depends on the suspended sediment concentration, it is in principle possible to infer the path-integrated sediment concentration from transmission measurements. This may be more

practically achievable with a bistatic geometry, with projector and receiver arrays on opposite sides of an estuary. However, since a monostatic detection model is being employed here to illustrate the concept, the monostatic case of co-located projector and receiver arrays on one side of the estuary, with a fixed target located on the far side is considered.

The system modelled here has a horizontally-projecting transmit array with a narrow (1° in both horizontal and vertical directions) beam and a source level of 220 dB re 1μPa. The receiver array is co-located with the projector and, for the purposes of these calculations, has the same beam pattern, although for a practical system a narrow projector beam and wide receiver beam may be more appropriate. The calculations have been carried out for a target with a target strength of 0 dB located at a range of 100 m and at the same depth as the sonar arrays. The water column is isovelocity before the effects of the bubble population on the phase speed are taken into account. The same depth-dependent bubble population employed to produce Figure 3 is used and, for simplicity, the suspended particle population is a depth-independent, unimodal suspension of 1μm particles of density 2600 kg m^{-3}.

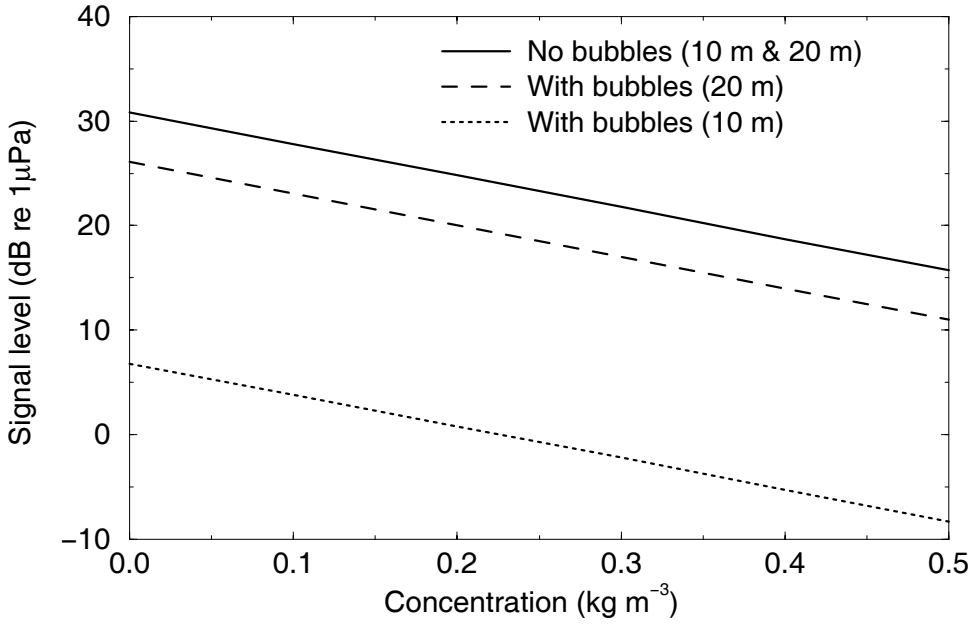

Figure 4. Variation in signal level with suspended particle concentration at two depths, with and without bubbles (see text).

Figure 4 shows how the level of the received signal varies with the mass concentration of suspended particles, with and without the chosen bubble population, for sensor / target depths of 10 m and 20 m. Only one line is plotted for the case where bubbles were not included in the calculations, as the results were essentially the same at the two depths in the absence of the bubbles. It is clear from this graph that even a calm water bubble population has a significant effect on the proposed measurement. At a sensor / target depth of 10 m the bubbles result in an additional reduction in the signal level of 24 dB. Even at a depth of 20 m the additional two-way transmission loss is 4.7 dB. The consequence of this is that if the effect of the bubbles is not taken into account a signal level of, say, 20 dB re 1 μPa might be taken to infer a path-averaged particle concentration of about 0.36 kg m^{-3}, whereas in fact that signal level in the presence of the bubble population corresponds to a concentration of 0.2 kg m^{-3}. In a practical measurement of this nature the effects of a static bubble population could be calibrated out. However it is likely that the bubble population may be sufficiently dynamic to preclude this. In such circumstances, care would be required to ensure that the interpretation of the measurements accounted for both the particle and bubble populations correctly. *A priori* knowledge of the bubble population may also be exploited to optimise transmission measurements of the form discussed here. For example, it is clear in this example that the effect of bubbles is greater near the surface, where their number density is highest. Therefore it would be best to locate the sonar at depth. Knowledge of the bubble size spectrum could also be exploited if, as for the bubble population considered in Section 5.2, there was found to be a frequency at which the contribution by bubbles to the overall attenuation was found to be a minimum.

6. Volume reverberation

In addition to contributing to volume attenuation, the presence of scatterers in the water column leads to increased volume reverberation. The amount of energy scattered by solid particles over the ranges of particle size and acoustic frequency of interest is small, but microbubbles scatter strongly and may therefore constitute a significant source of volume reverberation. A future enhancement to the sonar performance model will take this effect into account.

7. Conclusions

Expressions for calculating the excess attenuation due to dilute suspensions of suspended solid particles and microbubble populations and the phase speed in bubbly liquids have been given. These have been used to calculate the effect of dilute suspensions of natural, fine marine sediment particles on the acoustic attenuation coefficient and the effect of a natural population of bubbles on both the acoustic attenuation and phase speed. Results presented show that natural populations of fine grain suspended sediments can have a significant effect on the absorption coefficient at frequencies used by acoustic sensors, and natural bubble populations have a significant effect on both phase speed and attenuation at these frequencies.

The expressions for the excess attenuation by both suspended solid particles and microbubbles have been incorporated into the volume loss algorithm of a ray-based sonar performance model, with the excess attenuation taken into account in all propagating acoustic components (signal; surface, bottom and volume reverberation; and propagating noise terms) to calculate the resulting effect on the signal-to-noise ratio. The sound speed profile used in the model for calculating the ray paths is modified to take into account the effect of the bubbles on the phase speed. Results presented show that natural populations of both suspended particles and bubbles can significantly reduce the detection range for an active sonar operating in coastal waters.

A speculative technique is proposed to measure suspended sediment concentration flowing from the mouth of an estuary, over an acoustic path length of the order of 100 m. Preliminary model results show that, given a suitable experimental system, path averaged suspended particle concentrations could potentially be obtained from transmission measurements. It has also been demonstrated that the natural bubble population would need to be taken into account in any such measurement.

Conventional acoustic techniques for measuring suspended particle populations or bubble populations also employ high frequencies, ranging from hundreds of kHz to several MHz, operating over short ranges (<1m). It should be realised that, where both particles and bubbles may be present, the effects of particles need to be taken into account in interpreting bubble populations measurements and, conversely, the effects of bubbles should be taken into account in interpreting acoustic measurements of particle populations.

8. Acknowledgement

This work was carried out as part of Technology Group 01 of the MoD Corporate Research Programme.

References

[1] Urick RJ. The absorption of sound in suspensions of irregular particles. *J. Acoust. Soc. Am*. 1948; **20**: 283-289

[2] Sheng J and Hay AE. An examination of the spherical scatterer approximation in aqueous suspensions of sand. *J. Acoust. Soc. Am.* 1988; **83**: 598-610

[3] Commander KW and Prosperetti A. Linear pressure waves in bubbly liquids: comparison between theory and experiments. *J. Acoust. Soc. Am.* 1989; **85**: 732-746

[4] Fisher FH and Simmons VP. Sound absorption in seawater. *J. Acoust. Soc. Am*. 1977; **62**: 558-564

[5] Thorpe WH. Deep ocean sound attenuation in the sub and low kilocycle per second range. *J. Acoust. Soc. Am*. 1965; **42**: 648-654

[6] Francois RE and Garrison GR. Sound absorption based on ocean measurements: Part II: Boric acid contribution and equation for total absorption. *J. Acoust. Soc. Am.* 1982; **72**: 1879-1890

[7] Leighton TG, Simpson MD, Clarke JWL and Meers SD. A report on the development of an algorithm that incorporates depth dependence in the dispersion relation for bubbly media. ISVR Technical Report; **290**. 2000.

[8] Brown NR, Leighton TG and Richards SD. Measurement of the viscous sound absorption due to sediments suspended in water. In preparation for *IEEE Journal of Ocean Engineering.*

[9] Leighton TG, Phelps AD and Simpson MD. Oceanic bubble sizing: Measurements and proposed studies.

ISVR Technical Report; **273**. 1998

[10] Medwin H and Clay CS, Fundamentals of Acoustical Oceanography. Academic Press, San Diego, 1998.

[11] Medwin H. *In-situ* measurements of bubble populations in coastal waters. *J. Geophys. Res*. 1970; **75**: 599-611

[12] Medwin H. *In-situ* measurements of microbubbles at sea. *J. Geophys. Res*. 1977; **82**: 971-976

[13] Hall MV. A comprehensive model of wind generated bubbles in the ocean and predictions of the effects on sound propagation at frequencies up to 40 kHz. *J. Acoust. Soc. Am*. 1989; **86**: 1103-1116.